

Human scavenger protein AIM increases foam cell formation and CD36-mediated oxLDL uptake

Núria Amézaga,* Lucía Sanjurjo,* Josep Julve,^{†,‡} Gemma Aran,* Begoña Pérez-Cabezas,^{§,||} Patricia Bastos-Amador,^{§,||} Carolina Armengol,^{¶,‡} Ramon Vilella,** Joan Carles Escolà-Gil,^{†,‡} Francisco Blanco-Vaca,^{†,‡} Francesc E. Borràs,^{§,||} Annabel F. Valledor,^{††} and Maria-Rosa Sarrias^{*,‡,¶,1}

*Innate Immunity, [§]Innovation in Vesicles and Cells for Application in Therapy, and [¶]Liver Oncology Groups, Health Sciences Research Institute Germans Trias i Pujol, Badalona, Spain; ^{||}Department of Cell Biology, Physiology and Immunology, Universitat Autònoma de Barcelona, Spain; Centro de Investigación Biomédica en Red [†]de Diabetes y Enfermedades Metabólicas Asociadas y [¶]en el Área temática de Enfermedades Hepáticas y Digestivas, Barcelona, Spain; [†]Institut d'Investigacions Biomèdiques Sant Pau, Barcelona, Spain; ^{**}Laboratory of Immunobiology, Hospital Clínic de Barcelona, Spain; and ^{††}Nuclear Receptor Group, Department of Physiology and Immunology, School of Biology, University of Barcelona, Spain

RECEIVED DECEMBER 29, 2012; REVISED NOVEMBER 7, 2013; ACCEPTED NOVEMBER 7, 2013. DOI: 10.1189/jlb.1212660

ABSTRACT

AIM is expressed by macrophages in response to agonists of the nuclear receptors LXR/RXR. In mice, it acts as an atherogenic factor by protecting macrophages from the apoptotic effects of oxidized lipids. In humans, it is detected in atherosclerotic lesions, but no role related to atherosclerosis has been reported. This study aimed to investigate whether the role of hAIM extends beyond inhibiting oxidized lipid-induced apoptosis. To accomplish this goal, functional analysis with human monocytic THP1 cells and macrophages differentiated from peripheral blood monocytes were performed. It was found that hAIM reduced oxLDL-induced macrophage apoptosis and increased macrophage adhesion to endothelial ICAM-1 by enhancing LFA-1 expression. Furthermore, hAIM increased foam cell formation, as shown by Oil Red O and Nile Red staining, as well as quantification of cholesterol content. This was not a result of decreased reverse cholesterol transport, as hAIM did not affect the efflux significantly from [³H] cholesterol-laden macrophages driven by plasma, apoA-I, or HDL2 acceptors. Rather, flow cytometry

studies indicated that hAIM increased macrophage endocytosis of fluorescent oxLDL, which correlated with an increase in the expression of the oxLDL receptor CD36. Moreover, hAIM bound to oxLDL in ELISA and enhanced the capacity of HEK-293 cells expressing CD36 to endocytose oxLDL, as studied using immunofluorescence microscopy, suggesting that hAIM serves to facilitate CD36-mediated uptake of oxLDL. Our data represent the first evidence that hAIM is involved in macrophage survival, adhesion, and foam cell formation and suggest a significant contribution to atherosclerosis-related mechanisms in the macrophage. *J. Leukoc. Biol.* 95: 509–520; 2014.

Introduction

Macrophages play a central role in maintaining lipid homeostasis. Under homeostatic conditions, they differentiate from infiltrating monocytes in response to M-CSF, released by endothelial cells, and they are capable of ingesting circulating lipoproteins via the LDLR. Also, resident macrophages may secrete molecules that modify extracellular LDL, e.g., by oxidation (oxLDL), which is then recognized efficiently by scavenger receptors, such as SR-A and CD36 [1–3]. The latter is an 88-kDa transmembrane glycoprotein expressed in a wide variety of cell types, including macrophages [1]. The capacity of CD36 to bind and endocytose oxLDL was first demonstrated using a HEK-293 transfected with CD36 [4]. At present, extensive evidence corroborates these findings and shows that besides oxLDL [4], CD36 recognizes a wide variety of ligands, including bacterial cell-wall components [5] or apoptotic cells [6, 7], among others [1].

Abbreviations: 7-AAD=7-amino-actinomycin D, 9cRa=9cis-retinoic acid, ABC=ATP-binding cassette, ABCA1=ATP-binding cassette transporter A1, ABCG1=ATP-binding cassette transporter G1, acLDL=acetylated LDL, AIM=apoptosis inhibitor of macrophages, Alb=albumin, apoA-I=apolipoprotein A-I, CHX=cycloheximide, DiI=1,19-dioctadecyl-3,3,39,39-tetramethylindocarbocyanine perchlorate, FASN=fatty acid synthase, hAIM=human apoptosis inhibitor of macrophages, HDL=High density protein, HEK=human epithelial kidney cell line, HMDM=human monocyte-derived macrophage, IGTP=Institute Germans Trias i Pujol, LXR=liver X receptor, Mac-1=macrophage-1 antigen, mAIM=mouse apoptosis inhibitor of macrophages, MFI=mean fluorescence intensity, mLDL=modified LDL, oxLDL=oxidized LDL, qPCR=quantitative PCR, rt=room temperature, RXR=retinoid X receptor, siRNA=small interfering RNA, SR-A/B=scavenger receptor types A/B, SRCR=scavenger receptor cysteine-rich, T1317=T0901317

1. Correspondence: Health Sciences Research IGTP, Ctra Can Ruti, camí de les escoles s/n, Edifici de Recerca, Planta 1, 08916 Badalona, Spain. E-mail: mrsarrias@igtp.cat; Twitter: <http://www.twitter.com/mrsarrias>

Scavenger receptor-mediated oxLDL uptake may lead to cholesterol accumulation in the macrophage. Then, derived, intermediate products of the cholesterol biosynthetic pathway are known to activate the LXRs, transcription factors that belong to the nuclear receptor superfamily and that play key roles in maintaining lipid homeostasis. This is evidenced by observations that LXRs direct the expression of members of the ABC family of transporters, which has been implicated in mediating lipid efflux from a variety of cells, including macrophages. In particular, ABCG1 and ABCA1 transport intracellular cholesterol and phospholipids to HDL2 [8, 9] and to exogenous nascent plasma particles that contain lipid-poor acceptors, such as apoA-I [10], respectively. In this way, macrophages release cholesterol, which is mobilized from peripheral cells to the liver for its conversion to bile acids [11, 12].

Under persistent hyperlipidemic conditions, a series of changes in the vessel wall may lead to atherosclerosis, a chronic inflammatory condition in which macrophages play a key role. Accumulation of minimal oxLDL stimulates the overlying endothelial cells to produce a number of proinflammatory molecules, including adhesion molecules, such as ICAM-1, that will recruit monocytes to the arterial wall. In there, monocyte-derived macrophages accumulate excess cholesterol, thus becoming cholesterol-loaded foam cells that cluster in the sub-endothelial compartment [13]. This accumulation is not clinically significant but constitutes one of the initial steps in the development of atherosclerotic plaques [13, 14]. Complications of atherosclerosis, such as plaque rupture and thrombosis, are the most common causes of death in Western societies.

AIM, also named CD5 ligand, Sp α , and apoptosis inhibitor 6, is a macrophage-secreted glycoprotein that belongs to the SRCR superfamily of proteins [15]. It was identified as a downstream target gene of the LXR-RXR heterodimer in *in vivo* and *in vitro* mouse models [16, 17]. Several studies support the notion that mAIM prevents the apoptosis of macrophages and other cell types [18–20]. In this context, by using the LDLR-deficient mouse model of atherosclerosis, mAIM was defined as an atherogenic protein, as loss of mAIM expression lowered early lesion development by increasing macrophage apoptosis. Consistent with this observation, macrophage expression of mAIM facilitated macrophage survival within atherosclerotic lesions [18]. Interestingly, it was shown recently that mAIM is incorporated into adipocytes through CD36-mediated endocytosis [21]. Internalization of mAIM into adipocytes resulted in a reduction of the activity of cytosolic FASN [21, 22]. These results suggested that CD36 may function as a cellular receptor for mAIM.

The purpose of the present study was to determine whether hAIM contributes to key events of macrophage physiology in the context of atherosclerosis. Our findings in *in vitro* experiments point to an active role of hAIM in survival, cellular adhesion to endothelial ICAM-1 and VCAM-1, and foam cell formation and further suggest that hAIM binds to oxLDL and facilitates CD36-mediated oxLDL endocytosis. Therefore, hAIM is an active player in regulating macrophage lipid homeostasis and could contribute significantly to atherosclerosis-related mechanisms in the macrophage.

MATERIALS AND METHODS

Reagents and cells

PBS is 150 mM NaCl, 8 mM Na₂HPO₄, 1.5 mM KH₂PO₄, pH 7.4; TBS is 140 mM NaCl, 50 mM Tris-HCl, pH 7.4. Buffy coats, provided by the Blood and Tissue Bank (Barcelona, Spain), were obtained from healthy blood donors, following the institutional standard operating procedures for blood donation and processing. PBMCs were isolated by Ficoll-Paque (GE Healthcare, Piscataway, NJ, USA) density gradient centrifugation at 400 *g* for 25 min, and CD3+ cells were depleted by RosetteSep human CD3 depletion cocktail (Stemcell Technologies, Vancouver, BC, Canada). Recovered cells were washed twice in PBS and counted using Perfect-Count microspheres (Cytognos, Salamanca, Spain), as indicated by the manufacturer. Monocytes were obtained by positive selection using human CD14 MicroBeads and autoMACS columns (Miltenyi Biotec, Auburn, CA, USA) [23]. Differentiation of monocytes into HMDMs was allowed to occur spontaneously by adhesion of cells to the culture dishes, cultured in complete RPMI-1640 medium containing 10% AB human serum (Sigma-Aldrich, St. Louis, MO, USA), and by continued maturation for 14 days. To assess the effect of AIM on HMDMs, these were incubated with 1 μ g/ml endotoxin-free (<1.0 EU/1 μ g of the protein by the LAL method) rhAIM (R&D Systems, Abingdon, UK) or 1 μ g/ml control Alb, purified from human plasma (Grifols, Barcelona, Spain) for 24 h.

LDL and HDL purification and modification

Isolation of LDL and HDL fractions from plasma, plasma lipoprotein lipid, and apolipoprotein content analysis has been described in detail elsewhere [24, 25]. LDL, oxLDL, and acLDL were also purchased from Intracel (Frederick, MD, USA), so experiments were reproduced with both sources of LDL and mLDL with similar results.

Cell stimulation for gene-expression analysis and real-time qPCR

THP1 cells or HMDMs (1.5×10^6) from two different donors, matured for 7 days, were incubated for 24 h in RPMI medium containing fatty acid-free 3% BSA (Sigma-Aldrich), filtered previously through a 0.2- μ m sterile filter, and treated with 50 μ g/ml oxLDL (Intracel), T1317 (Tocris Bioscience, Bristol, UK), plus 9cRa (Sigma-Aldrich), 1 μ M each or DMSO (Sigma-Aldrich) alone. Cells were washed with PBS and total RNA extracted using the High Pure RNA Isolation Kit (Roche, Mannheim, Germany). Total RNA (1 μ g) was reverse-transcribed using the Transcriptor First Strand cDNA Synthesis Kit (Roche). Then, each RT reaction was amplified in a LightCycler 480 PCR system using the SYBR Fast Master Mix (KAPA Biosystems, Woburn, MA, USA). Samples were incubated for an initial denaturation at 95°C for 5 min, and then 40 PCR cycles were performed using the following conditions: 95°C for 10 s, 60°C for 20 s, and 72°C for 10 s. The following primer pairs were used: 5'-GACGAGAAGCAACCCTTCAG-3' and 5'-TCAAAGGGATCTTCACATTCGA-3' for hAIM; 5'-GAGAACTGT-TATGGGGCTAT-3' and 5'-TTCAACTGGAGAGGCAAAGG-3' for CD36; 5'-TCAGCTCCCAAGGGCTCTGTGC-3' and 5'-AAAGGCGCTTTGCCTG-GCCT-3' for SR-BI; 5'-TGAGCTACCCACCCTATGAACA-3' and 5'-CCCCT-GAACCAAGGAAGTG-3' for ABCA1; 5'-CCTGCTGTACTTGGGGATCGGGA-ACG-3' and 5'-CCAGCGCGGCAAAACAGCACAAAG-3' for ABCG1; 5'-CTC-CTTTGAGCTGTGTTGCAG-3' and 5'-CACCACATGCTTGCCATCC-3' for cyclophilin A. Gene-expression values were normalized to the expression levels of cyclophilin A. Fold-induction levels were calculated using as a reference the levels of expression of each gene at Time 0 for THP1-vector cells or those of untreated HMDMs.

Generation of stably transfected THP1-vector and THP1-hAIM cells

The cDNA of hAIM was obtained by reverse transcription of human spleen mRNA (Clontech, Mountain View, CA, USA) and subsequent PCR amplification with the following primers: 5'-CGCCGCTAGCGATGGCTCTGC-

TATTCCTCTT-3' (forward) and 5'-GCGCGGATCCCTATCCTGAGCAGAT-GACAG-3' (reverse). The amplified PCR product was cloned into the pGEM-T vector (Promega, Madison, WI, USA), *NheI*/*NotI*-restricted further, and cloned into appropriately digested pCI-neo vector (Promega), a kind gift of Dr. Margarita Martin (University of Barcelona, Spain). Subsequently, the human acute monocytic leukemia cell line THP1 (a kind gift of Dr. Alfonso del Rio, Fundació IGTP, Badalona, Spain) was transfected with *XmnI*-digested construct or empty pCI-neo vector using Amaxa (Lonza, Basel, Switzerland), following the manufacturer's instructions. Stably transfected THP1-vector and THP1-hAIM cells were selected in culture medium, supplemented with 500 $\mu\text{g}/\text{ml}$ geneticin (G418; Invitrogen, Paisely, UK).

Unless stated otherwise, THP1-vector and THP1-hAIM cells were differentiated to macrophages by incubation with 10 ng/ml PMA (Sigma-Aldrich) in RPMI 10% FBS medium for 48 h (referred as THP1 cells). The cell culture medium (Lonza) was supplemented with 100 U/ml penicillin and 100 $\mu\text{g}/\text{ml}$ streptomycin.

Analysis of hAIM protein expression

THP1 cells, HMDMs, or peripheral blood monocytes (1.5×10^6), differentiated in RPMI medium containing 1% FBS and 20 ng/ml M-CSF or GM-CSF (PeproTech) for 48 h, were incubated in RPMI 1% FBS or treated with oxLDL (50 $\mu\text{g}/\text{ml}$), T1317 (Tocris Bioscience), plus 9cRA (Sigma-Aldrich) 1 μM each or DMSO (Sigma-Aldrich), alone for 24 h. Analysis of hAIM expression was performed in cell lysates, as well as supernatants, as follows: cells were washed in cold PBS and lysed in lysis buffer [20 mM Tris (pH 7.5), containing 150 mM NaCl, 1 mM EDTA, 1 mM EGTA, 1% Triton X-100, 1 mM Na_3VO_4 (Sigma-Aldrich), complete protease inhibitor mixture tablets (Roche), and 1 mM PMSF] for 30 min at 4°C. Cell solubilizes were immunoprecipitated overnight at 4°C with 1 μg anti-hAIM mAb 18.2 (Santa Cruz Biotechnology, Santa Cruz, CA, USA), plus 20 μl 50% protein G-Sepharose beads (Sigma-Aldrich). Alternatively, the nuclei and cell debris were removed by centrifugation at 8000 g for 15 min, and protein concentration was measured with the BCA protein assay reagent kit (Pierce Perbio Science, Rockford, IL, USA), following the manufacturer's instructions. For secreted protein analysis, 1 ml serum-free culture supernatants was precipitated in 14% TCA and 0.14% Triton X-100 for 30 min at 4°C. The proteins were pelleted at 12,000 rpm for 30 min at 4°C, and washed with cold acetone. Monitoring of hAIM expression was performed by SDS-PAGE and Western blotting analysis. Precipitated proteins or 40–50 μg cell lysates were resolved in 10% SDS-polyacrylamide gels, electrophoretically transferred to nitrocellulose membranes (Bio-Rad Laboratories, Hertfordshire, UK), and blocked with Starting Block TBS blocking buffer (Pierce Perbio Science). The membranes were incubated overnight at 4°C with anti-hAIM-biotinylated polyclonal antibody (R&D Systems, Minneapolis, MN, USA) or anti- β -tubulin mAb (Sigma-Aldrich) diluted in blocking buffer. Appropriate fluorescently coupled secondary antibodies were added (IRDye680Cw-conjugated streptavidin or IRDye 800Cw-conjugated goat anti-mouse IgG; Li-Cor Biosciences, Lincoln, NE, USA) for 60 min at rt, and bound antibody was detected with an Odyssey Infrared Imager (Li-Cor Biosciences). Three 15-min washings between steps were performed with TBST (0.01% Tween 20). Densitometric analysis was performed by using the Odyssey V.3 software.

Apoptosis

THP1 cells or HMDMs, plated into 24-well culture plates (Nunc, Denmark) at 10^5 cells/well, were washed with PBS and incubated in RPMI 10% FBS for 48 h. To induce apoptosis, cells were treated with CHX (Sigma-Aldrich) at 100 $\mu\text{g}/\text{ml}$ for 6 h or oxLDL (5 or 100 $\mu\text{g}/\text{ml}$ for THP1 cells and 50 or 100 $\mu\text{g}/\text{ml}$ for HMDMs) for 24 h. Following treatment, cells were removed from plates with Accutase (PAA Laboratories, Somerset, UK), washed twice in ice-cold PBS, and stained with PE-conjugated Annexin V and 7-AAD, following the manufacturer's instructions (apoptosis detection kit; Becton Dickinson, Palo Alto, CA, USA). Cells were analyzed immediately with a FACSCanto II instrument and CellQuest software (Becton Dickinson). Apoptosis was expressed as the percentage of Annexin V-positive, 7-AAD-negative cells using untreated cells as a reference.

Flow cytometric analysis of CD11a, CD18, CD11b, and CD36 expression

THP1 cells or HMDMs (10^5) were washed with 3 ml PBS containing 2% FCS, 0.02% NaN_3 (washing buffer), at 4°C, and incubated with 1 μg anti-CD11a (Clone 33-1D2; Antibody Workshop II and IV), anti-CD18 (Clone 68-5A5; Antibody Workshop III), anti-CD11b (Clone ICRF44; BD Biosciences, Oxford, UK), or anti-CD36 (Clone 185-1G2; Antibody Workshop VI) mAb in washing buffer, supplemented with 10% human AB serum (labeling buffer) for 1 h at 4°C. The cells were washed once and incubated with FITC-conjugated anti-mouse IgG antibody (BD Biosciences), diluted 1/50 in labeling buffer for 45 min at 4°C. After washing, flow cytometric analysis was performed on a FACScan (BD Biosciences) with 10,000 events acquired for each sample.

Cell adhesion to ICAM-1 and VCAM-1

The wells of a 96-well plate (Nunc) were coated with 10, 5, or 2.5 $\mu\text{g}/\text{ml}$ human rICAM-1 or 1, 0.5, or 0.25 $\mu\text{g}/\text{ml}$ VCAM-1 (PeproTech, London, UK), as indicated, in endotoxin-free PBS (Grifols) overnight at 4°C. The wells were then washed three times with PBS, and nonspecific binding sites were blocked with 1% human Alb (Grifols) in RPMI 1640 for 1 h at 37°C. The wells were washed with PBS, and 5×10^5 cells in RPMI medium containing 2.5% FBS and 50 ng/ml PMA, in the presence or absence of 50 $\mu\text{g}/\text{ml}$ oxLDLs, were dispensed into triplicate wells at 37°C for 2 h and 30 min. For blocking experiments, cells were incubated for 30 min prior to addition to the plates with 2 μg endotoxin-free anti-CD11a (Clone H1111), 4 μg anti-CD11b (CBRM1/5), or mouse IgG1 K isotype control mAb (eBioscience, San Diego, CA, USA). After the incubation, nonadherent cells were removed by washing three times with warm (37°C) RPMI medium. Adhered cells were then fixed with 10% formaldehyde for 15 min and stained for 20 min with 0.1% crystal violet (Sigma-Aldrich). After excess dye was washed out three times with distilled water, the cell-bound dye was solubilized with 50 $\mu\text{l}/\text{well}$ 2% SDS. The absorbance at 590 nm was recorded on a Varioskan Flash microplate reader. Cell numbers were calculated against a standard curve of known concentrations. Nonspecific binding to Alb-coated wells was subtracted. In blocking experiments, data were plotted as percent of inhibition of cell adhesion to ICAM-1 of each cell line compared with isotype-matched, negative antibody control (IgG).

Quantification of foam cell formation

THP1 cells or HMDMs were incubated with 150 $\mu\text{g}/\text{ml}$ oxLDL for 24 h in RPMI 1% FBS or medium alone and subsequently stained with Oil Red O or Nile Red as follows. Cells were fixed in 10% (v/v) formalin (Sigma-Aldrich) for 1 h and washed with 60% (v/v) isopropanol. Dried cells were then stained with Oil Red O (0.5% Oil Red O in isopropanol:dH₂O 6:4) for 10 min. The cells were washed extensively with dH₂O and examined by light microscopy. For quantitative analysis, 10% formalin-fixed cells were incubated with a 1-mM solution of Nile Red (Molecular Probes, Life Technologies, Grand Island, NY, USA) in DMSO and washed extensively with cold PBS. Nile Red incorporation was analyzed by flow cytometry on a FACScan flow cytometer (BD Biosciences) with 10,000 events acquired for each sample.

Analysis of macrophage total and esterified cholesterol content

HMDMs were converted into foamy macrophages by incubation with 150 $\mu\text{g}/\text{ml}$ oxLDL or LDL in media containing 1% FBS for 24 h and [^3H] cholesterol (4 $\mu\text{Ci}/\text{ml}$; GE Healthcare). Lipid classes were separated by single-dimension, double-development TLC (Whatman, Merck, Germany), and the incorporation of [^3H]-labeled cholesterol was measured in a liquid scintillation 1500 Tri-Carb beta counter (PerkinElmer, Waltham, MA, USA), as described previously [24]. Cellular protein levels were determined using the BCA protein assay (Pierce Perbio Science). The data were expressed as cpm/mg cell protein.

Cholesterol efflux

THP1-vector and THP1-hAIM cells differentiated with 50 ng/ml PMA for 5 days [26], or HMDMs were converted into foam cells by incubation with oxLDL (150 μ g/ml) in RPMI media containing 1% FBS and [3 H] cholesterol (4 μ Ci/ml; GE Healthcare) for 24 h. The cells were then washed and incubated with RPMI medium containing 0.2% (v/v) fatty acid-free BSA for 24 h. After washing with PBS, the medium was replaced by RPMI containing 2% human plasma from healthy normolipemic subjects (total cholesterol <5.2 mmol/L; triglyceride <1 mmol/L) [24], 25 μ g/ml apoA-I (Sigma-Aldrich), or 25 μ g/ml HDL2 for 4 h. The medium was collected, and the cells were solubilized in 0.5 M NaOH overnight at 4°C. Radioactivity counts were determined in the medium and in the cellular fraction by using a 1500 Tri-Carb Packard scintillation counter. The percentage of cholesterol efflux was calculated as $100 \times (\text{cpm in the medium})/(\text{cpm in the medium} + \text{cpm in the cellular fraction})$. Total cellular protein levels were determined using the BCA assay (Pierce Perbio Science).

DiI-oxLDL uptake

Cells were incubated for the indicated times at 37°C with DiI-labeled oxLDL (DiI-oxLDL; Intracel) at the indicated concentrations in RPMI-1640 containing 0.2% (v/v) fatty acid-free BSA (Sigma-Aldrich). For competition analysis, a 40 \times molar excess of unlabeled oxLDL or Alb was added into the medium 1 h before the addition of 5 μ g/ml DiI-oxLDL, and cells were incubated for 12 h. After washing with PBS, cells were harvested by gentle scraping, and uptake was analyzed by flow cytometry on a FACScan flow cytometer (BD Biosciences) with 10,000 events acquired for each sample. To normalize the data, untreated control values (THP1-vector cells or HMDMs in the presence of Alb) were set to 100%, and then uptake data were calculated as percentage of DiI-oxLDL uptake versus controls.

Direct-binding ELISA assay

The assay was performed as described previously [27]. Briefly, 96-well plates (Nunc) were coated with oxLDL or BSA control protein at 2.5 μ g/ml in PBS overnight at rt. The remaining sites were blocked with PBS containing 5% nonfat milk for 1 h at 37°C. Several concentrations of rhAIM in PBS/1% nonfat milk were then added and incubated for 2 h at rt. The wells were washed with PBS/0.05% Tween-20, prior to addition of a 1/2000 dilution of biotin-labeled goat anti-hAIM (R&D Systems Abingdon, UK) in PBS/1% milk and incubation for 90 min at rt. The wells were washed, and HRP-conjugated streptavidin (Sigma-Aldrich), diluted 1/2000 in PBS/1% nonfat milk, was added for 30 min at rt. Unbound protein or antibody was washed three times between each step with PBS-0.01% Tween-20. Color was developed by adding 3, 3', 5', 5'-tetramethylbenzidine liquid substrate (Sigma-Aldrich), and the OD was read at 650 nm on a Varioskan Flash microplate reader.

CD36-mediated uptake of DiI-oxLDL

The cDNA-encoding, full-length human CD36 was synthesized by GenScript (Piscataway, NJ, USA) and subsequently cloned into appropriately digested pCI-neo vector (Promega). Subconfluent HEK-293 cells were transiently transfected with 4 μ g pCI-neo vector or pCI-neo-CD36 using 10 μ l TransFectin (Bio-Rad, Hercules, CA, USA), following the manufacturer's instructions. Two days after transfection, 50,000 cells were plated in the wells of a glass Millicell EZ Slide (Millipore, Billerica, MA, USA) with Alb or rhAIM at 1 μ g/ml and left to become foam cells by incubation for 24 h with 3 μ g/ml DiI-oxLDL in DMEM containing 5% FBS. Cells were fixed in 4% PFA, incubated in blocking buffer (PBS containing 3% BSA), and then incubated with 1 μ g anti-CD36 mAb 185-1G2, overnight at 4°C, followed by 40 μ g/ml Alexa Fluor 488 donkey anti-mouse IgG (Life Technologies) in PBS-3% BSA for another 30 min. Unbound antibodies were washed three times between each step with PBS. Cells were then mounted in Fluoromount medium (Sigma-Aldrich) and analyzed by fluorescence microscopy using a microscope (Zeiss AxioObserver Z1; Carl Zeiss, Germany), equipped with an AxioCam MRC 5 camera and AxioVision Rel. 4.8 software. The mean OD of DiI-oxLDL, as well as that of CD36, was quantified

using the ImageJ 1.46 software (W. S. Rasband, U.S. National Institutes of Health, Bethesda, MD, USA). Images from three independent assays (10–20 layers) were obtained. To avoid biased results, as a result of differential expression of CD36, only those fields with similar CD36 staining were considered for analysis. Moreover, DiI-oxLDL uptake was corrected for small differences in CD36 expression by dividing DiI-oxLDL/CD36 optical values. Data were expressed as percentages.

Silencing of CD36 expression and subsequent oxLDL uptake experiments

To silence CD36 cell-surface expression, undifferentiated THP1 cells were transfected with 20 nM of a set of four siRNAs targeting CD36 or an equal concentration of a nontargeting negative control pool (ON-TARGETplus SMARTpool siRNA; Dharmacon, Thermo Fisher Scientific, Waltham, MA, USA), by using INTERFERin (Polyplus, France) and following the manufacturer's instructions. Twenty-four hours later, the medium was replaced, and cells were differentiated with 50 ng/ml PMA in RPMI 10% FCS for 24 h, at which time-point, the medium was replaced with serum-free X-VIVO 15 medium (Lonza). Twenty-four hours later, cells were incubated with 5 μ g/ml DiI-oxLDL (Intracel) at 37°C for 3 h. After washing with PBS, cells were stained for CD36 expression with a specific antibody, as described above, harvested by gentle scraping, and uptake was analyzed by flow cytometry on a FACScan flow cytometer (BD Biosciences) with 10,000 events acquired for each sample. Data are shown as MFI of CD36, as well as DiI-oxLDL staining, and are representative of two independent experiments performed in duplicate.

C75 treatment of THP1 cells and determination of CD36, CD11a, and CD11b cell-surface expression

THP1-vector cells were treated with 6.25 μ g/ml C75 (Cayman Chemical, Ann Arbor, MI, USA), diluted in DMSO or an equal dilution of DMSO as a negative control, in RPMI 10% FCS for 24 h. Cells were then analyzed for CD36, CD11a, and CD11b expression, as detailed above.

Statistical analyses

The results are expressed as mean \pm SEM. Statistical analyses were performed with the Graphpad Prism V.5 software using the Student's *t*-test. Values of *P* \leq 0.05 were considered significant.

RESULTS

Induction of hAIM expression by oxLDL and LXR/RXR agonists and protection of macrophages from oxLDL-induced apoptosis

Several groups have reported that mAIM mRNA is markedly induced in macrophages when cells are incubated with oxLDL [18] or LXR/RXR synthetic agonists [16–18]. As shown in **Fig. 1A**, we observed a similar response in HMDMs. Interestingly, PMA-treated THP1 cells failed to up-regulate hAIM mRNA in response to oxLDL but did enhance its mRNA synthesis upon LXR/RXR activation. We next examined oxLDL and LXR/RXR agonist-regulated protein expression and could not detect hAIM in either type of cell (data not shown). Only when macrophages were differentiated with M-CSF or GM-CSF did they express low levels of hAIM protein and show enhanced hAIM protein content upon treatment with oxLDL or T1317 + 9cRA (**Fig. 1B**).

To overcome the limitation of absent (or undetectable) hAIM protein expression, we generated a macrophage cell line, stably expressing hAIM (THP1-hAIM). Validation of hAIM expression in antibiotic-resistant THP1 clones was per-

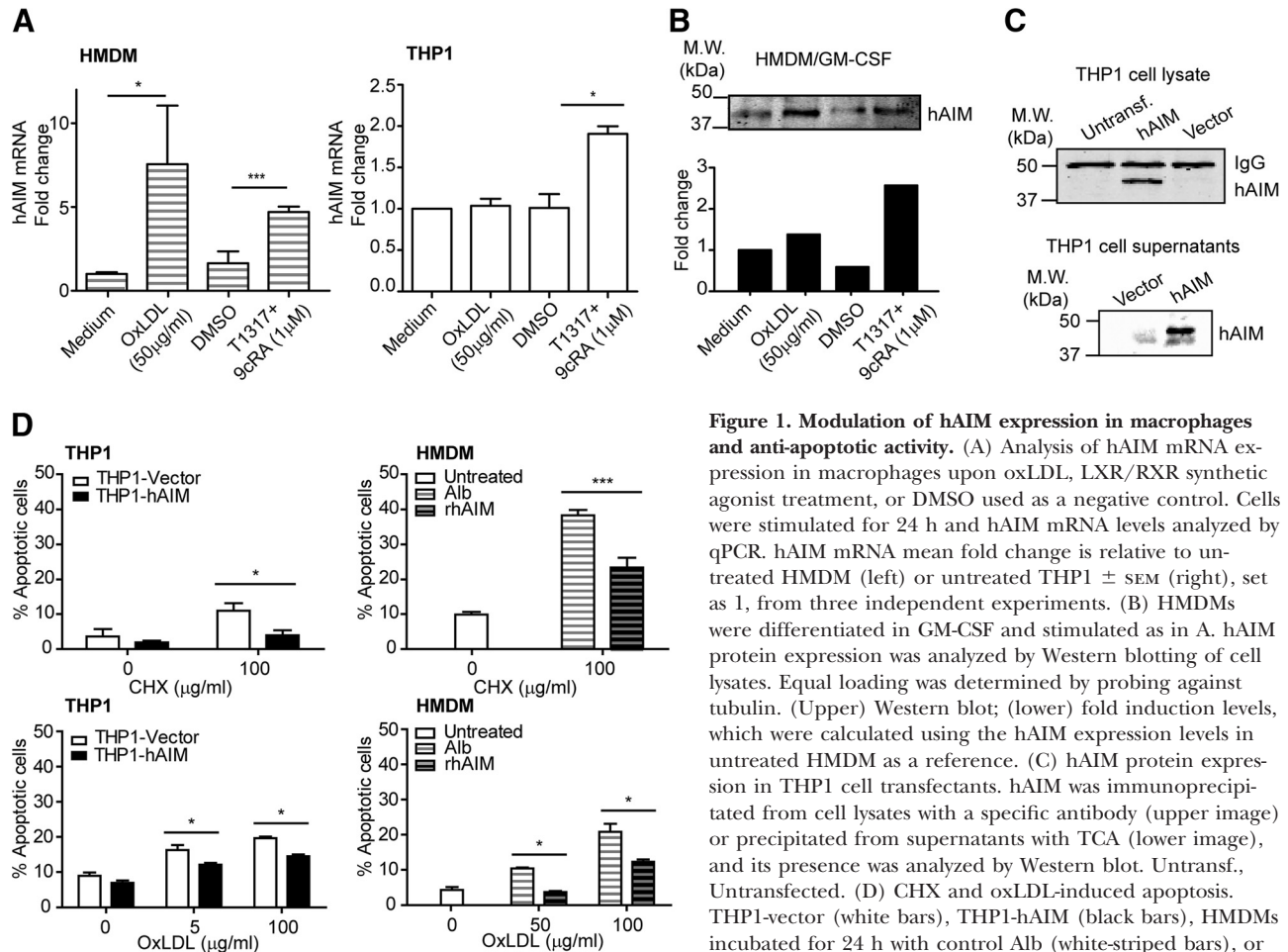


Figure 1. Modulation of hAIM expression in macrophages and anti-apoptotic activity. (A) Analysis of hAIM mRNA expression in macrophages upon oxLDL, LXR/RXR synthetic agonist treatment, or DMSO used as a negative control. Cells were stimulated for 24 h and hAIM mRNA levels analyzed by qPCR. hAIM mRNA mean fold change is relative to untreated HMDM (left) or untreated THP1 \pm SEM (right), set as 1, from three independent experiments. (B) HMDMs were differentiated in GM-CSF and stimulated as in A. hAIM protein expression was analyzed by Western blotting of cell lysates. Equal loading was determined by probing against tubulin. (Upper) Western blot; (lower) fold induction levels, which were calculated using the hAIM expression levels in untreated HMDM as a reference. (C) hAIM protein expression in THP1 cell transfectants. hAIM was immunoprecipitated from cell lysates with a specific antibody (upper image) or precipitated from supernatants with TCA (lower image), and its presence was analyzed by Western blot. Untransf., Untransfected. (D) CHX and oxLDL-induced apoptosis. THP1-vector (white bars), THP1-hAIM (black bars), HMDMs incubated for 24 h with control Alb (white-striped bars), or rhAIM (black-striped bars) were incubated with medium

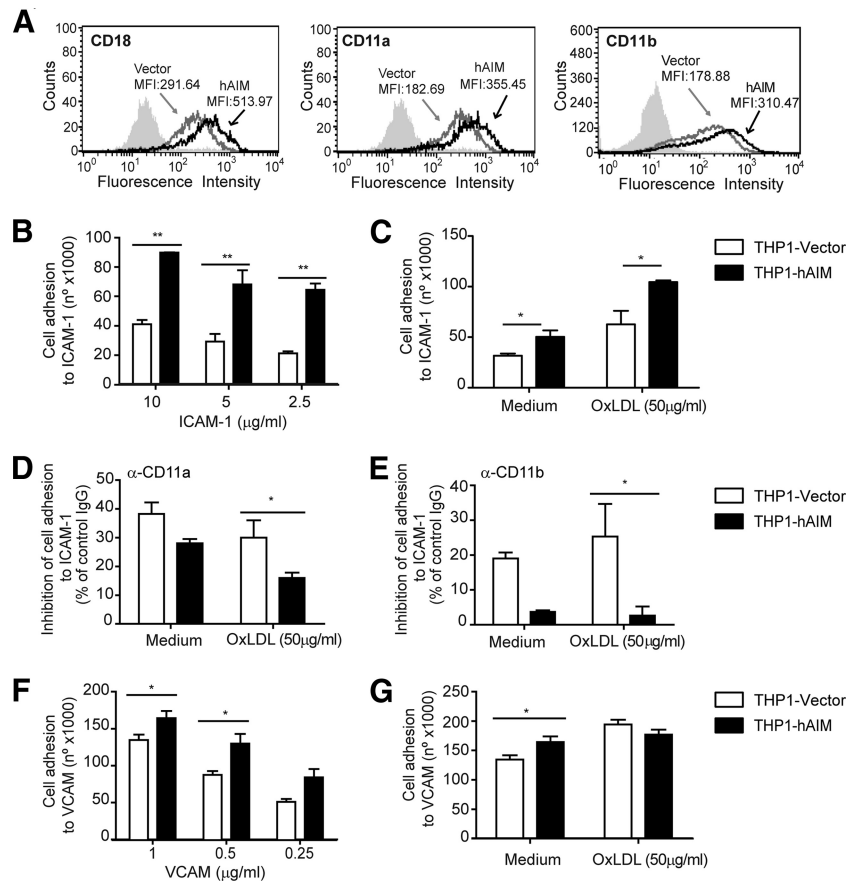
alone or medium supplemented with the indicated concentrations of CHX for 6 h or oxLDL for 24 h. Apoptosis was assessed using Annexin V and 7-AAD staining and analyzed by flow cytometry. Results are expressed as the percentage of apoptotic cells (Annexin V-positive, 7-AAD-negative cells). * $P \leq 0.05$; *** $P \leq 0.001$; t -test.

formed by Western blot (Fig. 1C). In these assays, a band of 38kDa was detected with a specific mAb in THP1-hAIM cell lysates (upper panel), as well as cell supernatants (lower panel), thus indicating correct expression and secretion of the protein. As expected, no hAIM expression was observed in the control THP1-vector cell line. As previous studies demonstrated that mAIM protects macrophages from the apoptotic effects of oxidized lipids in vitro [18], we analyzed whether hAIM conferred resistance to macrophage apoptosis induced by oxLDL and a well-known apoptotic agent—the protein synthesis inhibitor, CHX. Stable THP1 cell transfectants or HMDMs were incubated with oxLDL or CHX, and apoptosis was measured by Annexin V and 7-AAD staining. In these assays, the presence of hAIM conferred resistance to the apoptotic effect of CHX, as well as oxLDL (Fig. 1D). This is reflected by a lower percentage of apoptotic cells in THP1-hAIM and HMDM incubated with rhAIM than in control THP1-vector cells or HMDMs in the presence of Alb. These data support the notion that in human and mouse, AIM acts as an antiapoptotic molecule and that its transcription is induced in HMDM by oxLDL, as well as LXR/RXR agonists. These data also suggest a highly regulated control of hAIM protein synthesis.

hAIM increases macrophage adhesion to ICAM-1 by enhancing the expression of LFA-1 and Mac-1

ICAM-1 is expressed in atherogenic lesions and regulates monocyte adhesion to the arterial endothelial surface and migration into the subendothelial space [28]. Interaction with the integrin LFA-1 is a key step in these processes. Characterization of THP1-hAIM cell transfectants by flow cytometry staining showed increased cell-surface expression of LFA-1. More precisely, MFI staining values of the two integrins that form the LFA-1 heterodimer—CD11a and CD18—were two-fold in THP1-hAIM cells compared with those of the THP1-vector (Fig. 2A). CD18 is also able to dimerize with CD11b to form Mac-1, which is also a ligand of ICAM-1 [29]. We therefore assessed expression of CD11b and found that it was also increased in THP1-hAIM cells (Fig. 2A). We hypothesized that this could confer hAIM-expressing cells with enhanced adhesion capacity to the adhesion molecule ICAM-1. Experiments were performed in which THP1 cell transfectants were allowed to adhere to a recombinant form of the ectodomain of ICAM-1 or Alb-coated plates and bound cells stained with crystal violet. hAIM expression increased THP1 cell attachment to ICAM-1

Figure 2. THP1-hAIM cells show increased expression of CD11a, CD18, and CD11b and cellular adhesion to ICAM-1. (A) Cell-surface expression of CD18, CD11a, and CD11b in THP1 cell transfectants. Shaded histograms indicate IgG-matched, isotype-negative control. Representative histograms of three independent experiments with similar results. (B–G) THP1 cells were added to ICAM-1, VCAM-1, or Alb-coated wells for 2.5 h. Nonadherent cells were removed by extensive washing, and remaining cells were stained with crystal violet. Adherence was quantitated using a standard curve of known input cell numbers. Binding to Alb-coated plates was a measure of nonspecific cell attachment and was subtracted. (B) THP1 cell binding to different concentrations of immobilized ICAM-1. (C) THP1 cells in the presence or absence of 50 $\mu\text{g}/\text{ml}$ oxLDL were added to plates containing 2.5 $\mu\text{g}/\text{ml}$ immobilized ICAM-1. (D and E) Cells were preincubated with blocking antibodies to CD11a (D) or CD11b (E), or an isotype-matched IgG, used as a negative control prior to adhesion to ICAM-1, immobilized at 5 $\mu\text{g}/\text{ml}$. Data were plotted as the percent of inhibition of cell adhesion to ICAM-1 of each cell line compared with an isotype-matched negative control antibody. (F) THP1 cell binding to different amounts of immobilized VCAM-1. (G) THP1 cells in the presence or absence of 50 $\mu\text{g}/\text{ml}$ oxLDL were added to plates containing 0.5 $\mu\text{g}/\text{ml}$ immobilized VCAM-1. Results are representative of four independent experiments. * $P \leq 0.05$; ** $P \leq 0.01$; t -test.



by twofold, consistent with the enhanced expression of LFA-1 in these cells (Fig. 2B). Binding specificity to ICAM-1 was demonstrated by control experiments, in which THP1-vector and THP1-hAIM cell adhesion to ICAM-1 was approximately fourfold that of Alb control (data not shown) and by the dose-dependent response of the interaction (Fig. 2B). After 2.5 h incubation with oxLDL, THP1-vector and THP1-hAIM cell lines doubled their capacity to adhere to ICAM-1 (Fig. 2C). In blocking experiments, a blocking antibody to CD11a was able to inhibit binding of THP1-vector cells to ICAM-1 to 40%, compared with an isotype-matched antibody control, in the presence or absence of oxLDL (Fig. 2D). The inhibitory effect of this antibody was reduced by approximately one-half in THP1-hAIM-expressing cells, in accordance with the doubled surface expression of CD11a in these cells. Likewise, a blocking antibody to CD11b inhibited binding of THP1-vector cells to ICAM-1 by 20% in the presence or absence of oxLDL. Interestingly, no significant blocking of this antibody could be observed when THP1-hAIM cells were assayed (Fig. 2E), suggesting higher affinity of Mac-1 to ICAM-1 in these cells versus THP1-vector cells.

We next assessed whether hAIM-expressing cells also showed enhanced binding to VCAM-1, which is also up-regulated in endothelial cells in lesions [30]. Interestingly, dose-response binding experiments showed that untreated THP1-hAIM cells bound better than THP1-vector cells to VCAM-1 (Fig. 2F). However, binding to VCAM-1 was equal in both cell types

upon oxLDL treatment (Fig. 2G). Altogether, the data suggest that hAIM-expressing cells have a higher capacity to promote macrophage-endothelial cell adhesion.

hAIM increases foam cell formation

We next assessed whether the presence of hAIM alters oxLDL-induced foam cell formation. Foam cells are generated by enhanced cytoplasmic storage of cholesteryl esters and triglycerides. These can be visualized by staining with the lipid-specific dyes Oil Red O (for microscopic examination) and Nile Red (for flow cytometry quantification). THP1 cells and HMDMs were treated with oxLDL for 24 h, and cells were subsequently stained. THP1-hAIM cells presented higher Oil Red O staining than control THP1-vector cells (Fig. 3A, left). Similarly, HMDMs accumulated higher amounts of lipids when rhAIM was added to the culture compared with Alb (Fig. 3A, right). Assessment of cellular lipid accumulation by flow cytometry analysis of Nile Red-stained foamy macrophages yielded similar results, and the amount of lipid was higher in hAIM-expressing cells (Fig. 3B). These data were confirmed further by quantification of total and esterified cholesterol in HMDMs by TLC separation and scintillation counting. rhAIM was observed to enhance total and esterified cholesterol contents in oxLDL-treated HMDMs compared with control Alb (Fig. 3C). Overall, the data strongly indicate that hAIM increases foam cell formation.

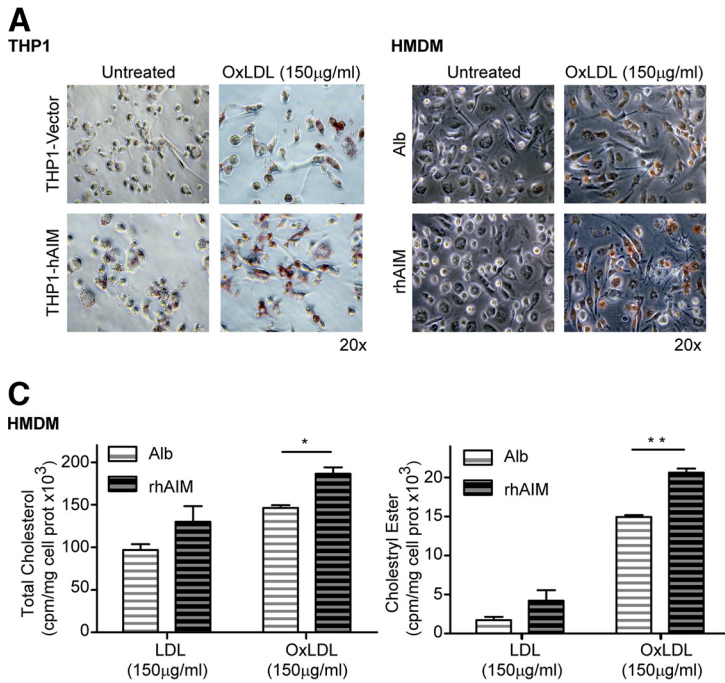


Figure 3. hAIM enhances foam cell formation. THP1 cells or HMDMs were treated with 150 µg/ml oxLDL for 24 h. Lipid content was examined as follows: (A) THP1 cells (left) or HMDMs (right) were fixed and stained with Oil Red O and observed by light microscopy. (B) THP1 cells were stained with Nile Red and analyzed by flow cytometry. (Left) Data from three experiments are shown, in which values are expressed relative to untreated THP1-vector cells (set as 1). (Right) Representative histogram of fluorescence intensity of Nile Red staining on oxLDL-treated THP1 cells. (C) Total cholesterol (left) and cholesteryl esters (right) in HMDMs. HMDMs from three donors were incubated for 24 h with control Alb (white-striped boxes) or with rhAIM (black-striped boxes) and then loaded with 150 µg/ml oxLDL in

the presence of [³H] cholesterol, and TLC cellular cholesterol fractions were analyzed by liquid scintillation. Total cholesterol is the sum of free and esterified cholesterol. prot, Protein. **P* ≤ 0.05; ***P* ≤ 0.01; *t*-test.

hAIM does not play a major role in macrophage cholesterol efflux

It is well-known that foam cell generation is driven by an imbalance between the uptake and efflux of cholesterol by macrophages [31]. Given the capacity of hAIM to induce foam cell formation, we next questioned whether its presence modifies either of these two processes, as well as the expression of the key genes involved. Cholesterol efflux from macrophages is mainly directed by members of the ABC transporter family, such as ABCA1 and ABCG1, through active, reverse-cholesterol transport, in a process that requires the presence of cholesterol acceptors apoA-I or HDL, respectively [32]. SR-BI is a

dual transporter that mediates enhanced bidirectional-free cholesterol flux between cells and extracellular acceptors [33]. We determined whether hAIM modulates mRNA expression of ABCA1, ABCG1, and SR-BI by real-time PCR in THP1 cells. The levels of ABCA1 mRNA were similar in THP1-vector versus THP1-hAIM cells (Fig. 4A). Treatment with oxLDL increased ABCA1 expression in both cell lines. In contrast, ABCG1 mRNA levels were higher in hAIM-expressing cells and increased further upon oxLDL stimulation. SR-BI mRNA expression increased in THP1-vector cells by oxLDL addition and reached similar levels to those of THP1-hAIM cells, which remained unchanged.

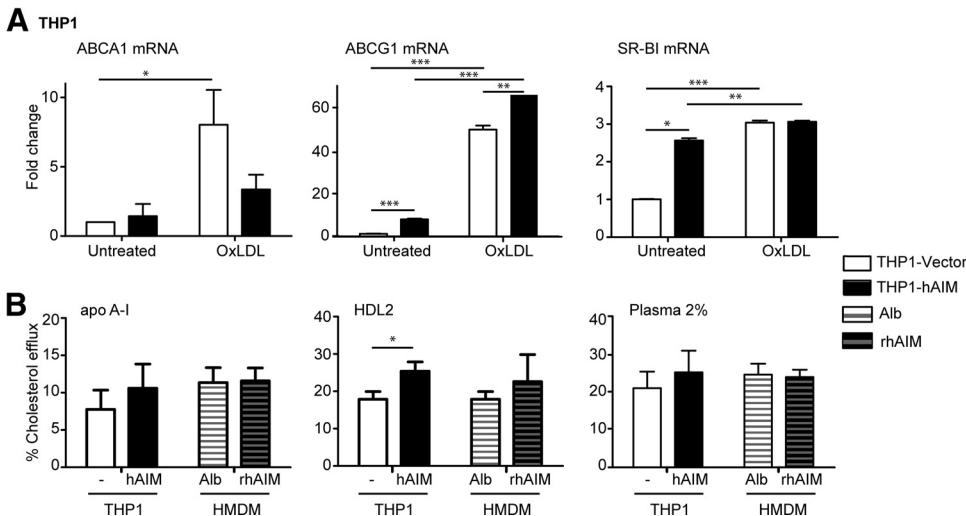


Figure 4. hAIM in macrophage cholesterol efflux. (A) THP1 cells were incubated with 50 µg/ml oxLDL for 24 h, and the amount of mRNA encoding ABCA1, ABCG1, and SR-BI was measured by qPCR (data show mean fold change relative to untreated THP1-vector ± SEM from three independent experiments). (B) Cholesterol efflux from THP1 cell transfectants and HMDMs in the presence rhAIM. [³H] Cholesterol efflux was measured after a 4-h incubation with apoA-I (25 µg/ml), HDL2 (25 µg/ml) and human plasma (2%). The graphics show mean levels ± SEM from three independent experiments. **P* ≤ 0.05; ***P* ≤ 0.01; ****P* ≤ 0.001; *t*-test.

To assess further whether hAIM-enhanced ABCG1 expression results in changes in cholesterol efflux rates, acLDL-loaded THP1 cells or HMDMs were incubated with [3 H] cholesterol, and the capacity of whole plasma, apoA-I, or HDL2 to induce cholesterol efflux was evaluated. THP1 cell cholesterol efflux to human plasma was dose-dependent (data not shown). This observation demonstrates the specificity/sensitivity of the assay. Expression of hAIM did not alter cholesterol efflux in these assays. Likewise, cholesterol efflux to 2% human plasma and apoA-I in THP1 cells and HMDMs was not modified by hAIM (Fig. 4B). When HDL2 was used as the acceptor, a slight increase in cholesterol efflux in THP1-hAIM cells versus THP1-vector cells was detected. This result was not reproduced in HMDMs. Overall, our data suggest that hAIM does not have a major impact on macrophage cholesterol efflux.

hAIM enhances macrophage oxLDL uptake, binds to oxLDL, and facilitates CD36-mediated oxLDL endocytosis

We then studied whether hAIM enhances oxLDL uptake. For this purpose, THP1 cell transfectants or HMDMs were incubated with a range of concentrations of fluorescently labeled oxLDL (DiI-oxLDL) over different periods, and fluorescence uptake was analyzed by flow cytometry. **Figure 5A** shows that hAIM increased the uptake of oxLDL significantly in both types of cell. The uptake was specific, as it was competed by a molar excess of nonlabeled oxLDL but not Alb (data not shown). Our results suggest that hAIM enhances macrophage oxLDL uptake.

As CD36 is one of the major scavenger receptors for oxLDL in macrophages [1] and given that mAIM binds to cell-surface CD36 [21], we hypothesized that hAIM may be increasing oxLDL uptake by modulating CD36 expression and/or activity. In this regard, real-time PCR analysis revealed that THP1-hAIM cells show greater CD36 expression than THP1-vector cells (Fig. 5B, left). Moreover, and as published before [34, 35], treatment with oxLDL enhanced CD36 mRNA in both cell lines, but this increase was significantly greater in THP1-hAIM cells. Cellular staining with a specific mAb and subsequent flow cytometry analysis revealed that hAIM increased cell-surface CD36 expression in THP1 cells and HMDMs (Fig. 5B, right).

We first analyzed whether hAIM interacts directly with oxLDL in a direct ELISA assay. OxLDL- or BSA (negative control)-coated wells were incubated with a range of concentrations of rhAIM, and the binding of this protein was detected with a specific antibody. Interestingly, rhAIM showed a dose-dependent and saturable binding to oxLDL (Fig. 5C).

We next tested the possibility that hAIM may be enhancing CD36-mediated oxLDL uptake in a widely used *in vitro* system [2, 4]. Empty vector- or CD36-transfected HEK-293 cells were incubated with DiI-oxLDL for 24 h, with the presence of rhAIM or Alb as control and uptake analyzed by fluorescence microscopy. As expected, HEK-293 cells transfected with empty vector did not show major staining, indicating low or negative oxLDL endocytic capacity (data not shown). This response was not altered upon addition of rhAIM, suggesting the requirement of a cell-surface receptor for hAIM-mediated enhanced

uptake (data not shown). On the contrary, expression of CD36 rendered the cells with oxLDL endocytic capacity. When CD36-expressing cells were treated with rhAIM, a significant increase in oxLDL uptake compared with control Alb-treated cells was appreciated (Fig. 5D). Our results suggest that hAIM serves to facilitate CD36-mediated uptake of oxLDL on CD36-expressing HEK-293 cells. We then performed experiments with oxLDL uptake after CD36 silencing in THP1 cells to verify this hypothesis. Transfection of a pool of siRNAs targeting CD36 lowered its cell-surface expression by 40% in THP1-vector cells and by 50% in THP1-hAIM cells compared with the negative control, nontargeting siRNA pool. In both cases, this resulted in a 20% reduction of oxLDL uptake in these cells. These data reinforced the notion that oxLDL uptake mediated by hAIM is mediated through CD36.

Inhibition of FASN activity does not account for CD18, CD11a, CD11b, and CD36 overexpression in THP1-hAIM cells

Given that CD36, CD18, CD11a, and CD11b overexpression in THP1-hAIM cells occurs independently of oxLDL lipid uptake, we questioned whether this could be a result of hAIM down-modulation of FASN activity in macrophages [22]. However, when THP1-vector cells were treated with C75, a synthetic FASN inhibitor, cell-surface expression of CD36 was not altered, whereas that of CD18, CD11a, and CD11b was diminished significantly (**Fig. 6**). Therefore, these results suggest that inhibition of FASN in the THP1 cell line is not concomitant with the effect of hAIM in these cells.

DISCUSSION

The present report shows that hAIM participates in several key aspects of atherosclerosis-related mechanisms in the macrophage. This finding is of relevance, as although previous studies have shown that mAIM is involved in preventing macrophage apoptosis [18], we have extended our knowledge of this molecule, and our data support the notion that hAIM makes a relevant contribution to macrophage protection from apoptosis, cellular adhesion, and promotion of lipid accumulation through enhanced CD36-mediated uptake.

AIM mRNA is synthesized in the same human and mouse tissues (spleen, LN, thymus, bone marrow, liver, and fetal liver). However, three AIM mRNA transcripts expressed by human lymphoid tissues contrast with the single mRNA transcript found in the mouse, probably reflecting differences in mRNA regulation in these two species [36, 37]. At the amino acid level, they are highly homologous (69% identity, 80% similarity), and their predicted MW is 37 kDa; however, there are species-specific differences in their glycosylation patterns [38] that may result in distinct activities. In this regard, a recent publication confirmed the relevance of glycosylation in mAIM function, by reporting that mutation of two N-glycosylation sites in the protein inhibited its secretion and enhanced its lipolytic function in adipocytes [39]. Therefore, it was worth analyzing whether key functions described already for mAIM, related to atherogenesis, were conserved in hAIM. In this re-

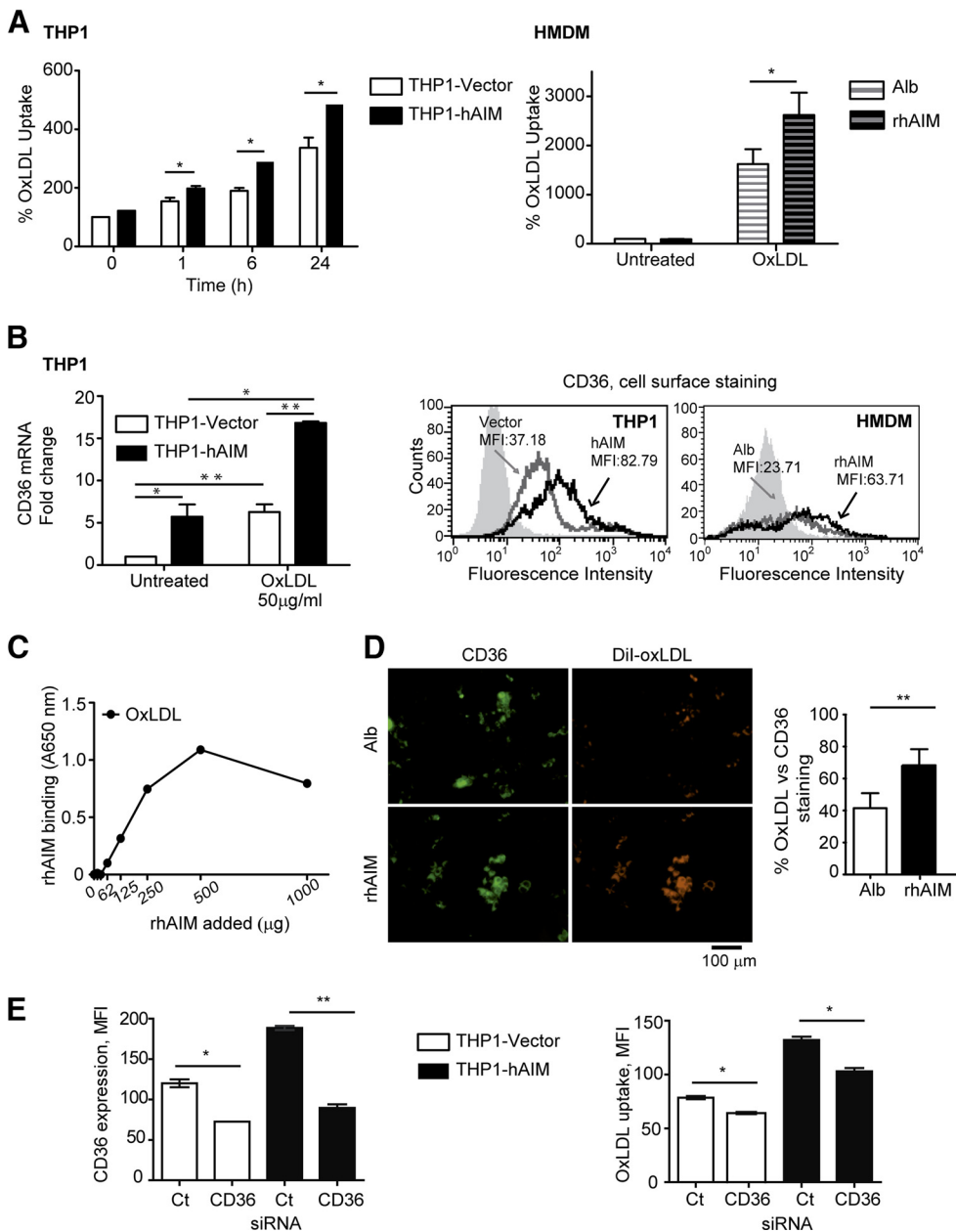


Figure 5. hAIM in oxLDL uptake by macrophages. (A) OxLDL uptake. DiI-oxLDL (1 µg/ml) was added to THP1 cells or HMDMs in the presence of rhAIM or Alb for the indicated times, and uptake was analyzed by flow cytometry. Untreated control values (THP1-vector cells or HMDMs in the presence of Alb) were set to 100%, and then uptake data were calculated as percentage of DiI-oxLDL uptake versus controls. Graphs depict the percentage of DiI-oxLDL uptake of at least three independent experiments. (B) Analysis of CD36 expression. (Left) THP1 cells were incubated with 50 µg/ml oxLDL for 24 h, and the amount of mRNA encoding CD36 was measured by qPCR (mean fold change relative to untreated THP1-vector cells from three independent experiments). (Right) Flow cytometry analyses of THP1 and HMDM CD36 cell-surface expression in the absence of oxLDL. Staining with negative control antibody is shown in shading. (C) ELISA showing direct binding of hAIM to oxLDL. BSA control protein or oxLDL was immobilized on a plate and incubated with several concentrations of rhAIM. rhAIM binding was detected with a specific biotinylated polyclonal antibody, followed by Streptavidin-Peroxidase labeling. Data are from a single experiment, representative of three individual experiments. (D) OxLDL uptake via CD36. (Left) HEK-293 cells were transiently transfected with CD36 and incubated with 3 µg/ml DiI-oxLDL in the presence of rhAIM (1 µg/ml) or Alb as a negative control. Cells were washed and fixed with PFA 4%, stained with an anti-CD36-specific mAb, and analyzed by fluorescence microscopy. Representative photomicrographs are shown. (Right) The mean OD of DiI-oxLDL, as well as that of CD36, was quantified using the ImageJ software from three independent assays (10–20 layers each). Percentage of DiI-oxLDL

staining was calculated as a ratio between the DiI-oxLDL mean OD and that of CD36 for each photomicrograph $\times 100$. (E) Effect of silencing of CD36 in oxLDL uptake. THP1 cells were transfected with siRNA targeting CD36 or a nontargeting negative control (Ct) and incubated with 5 µg/ml DiI-oxLDL for 3 h at 37°C. CD36 expression (left) as well as DiI-oxLDL uptake (right) were analyzed by flow cytometry and are expressed as MFI. Data are the mean of duplicates of a representative experiment performed twice. * $P \leq 0.05$; ** $P \leq 0.01$; t -test.

gard, similarly to mAIM, low levels of hAIM mRNA could be detected by real-time PCR, in THP1 cells or HMDMs from several donors used for our studies. Treatment with oxLDL or LXR/RXR synthetic agonists T1317 and 9cRa induced up-regulation of hAIM mRNA expression in HMDMs, suggesting a conserved control of AIM transcription. However, although LXR/RXR activation raised hAIM mRNA levels in the THP1 cell line, oxLDL treatment failed to do so. This cell line is a widely accepted model for the study of macrophage lipid homeostasis. In fact, our data on THP1 cellular adhesion, foam

cell formation, as well as lipid efflux and uptake are in agreement with previous results. Defective hAIM mRNA up-regulation by this cell line deserves further investigations.

In any case, we did not detect hAIM expression at the protein level in THP1 or HMDMs, indicating low or null protein translation (data not shown). hAIM protein expression was detected only when HMDMs were differentiated with macrophage-associated CSFs, namely M-CSF or GM-CSF. These are key cytokines involved in the survival, proliferation, and differentiation of myeloid progenitor cells, as well as in the func-

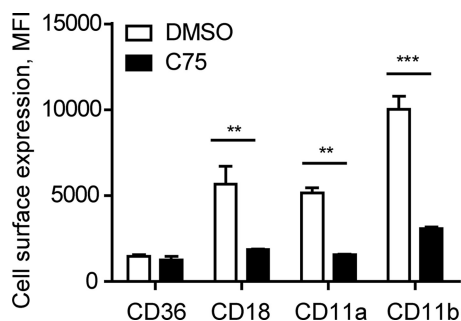


Figure 6. Effect of FASN inhibition on THP1-vector cell CD36, CD18, CD11a, and CD11b expression. THP1-vector cells were treated with C75, a synthetic FASN inhibitor for 24 h, or with DMSO as a negative control, and cell-surface receptor expression was subsequently analyzed by flow cytometry. Data are the mean of duplicates of a representative experiment performed twice. $**P \leq 0.01$; $***P \leq 0.001$; two-way ANOVA.

tional activation of mature myeloid cells. Furthermore, both cytokines have emerged as key factors in the pathogenesis of atherosclerosis [40]. Previous reports suggested that expression of mAIM requires a specific tissue microenvironment, as its expression diminishes in cultured cells [16, 41]. In this sense, our data show that macrophage differentiation with CSFs allows hAIM translation *in vitro*. OxLDL or LXR/RXR agonist addition to CSF-treated HMDMs induced an increase in hAIM cellular protein levels. Our data are consistent with previous findings showing that the macrophages of human atherosclerosis lesions show high hAIM expression [18].

To assess hAIM function, rhAIM was added to the primary cell cultures throughout the present study. Moreover, a THP1 cell line, stably expressing hAIM, was generated. With the use of this cell line we assessed initially whether the antiapoptotic activity of mAIM is conserved in hAIM. THP1-hAIM cells as well as HMDMs incubated with rhAIM were more resistant, not only to CHX but also to oxLDL-induced apoptosis. Noteworthy, in our hands, addition of oxLDL consistently induced apoptosis to THP1 cells, although to a maximum of 20% apoptosis. In contrast, we only detected oxLDL-induced apoptosis in HMDM in one out of the four different donors tested (data not shown). Although it is widely accepted that oxLDL induces macrophage apoptosis [42], data from several laboratories have shown that under certain conditions, oxLDL can be antiapoptotic in this cell type as a result of the effect of CSFs [43–45]. The lack of CSF addition to the HMDM culture medium may explain the heterogeneity in HMDM responses that we observed. Nevertheless, our findings suggest that mAIM-mediated protection of macrophages from the apoptotic effects of oxidized lipids *in vitro* [18] is conserved in the human form.

Foam cell accumulation in the arterial wall and subsequent plaque formation and stabilization involve active participation of macrophage integrin-endothelial receptor contacts, such as LFA-1 (CD11a/CD18) and Mac-1 (CD11b/CD18) with ICAM-1 (CD54) [46]. In fact, oxLDL has been shown to enhance ICAM-1 expression in endothelial cells [47]. Our data showed

increased THP1-hAIM cell attachment to ICAM-1-coated plates, which correlated with higher LFA-1 as well as Mac-1 expression in these cells. Interestingly, hAIM also conferred macrophages with enhanced adhesion capacity to VCAM-1, which is also up-regulated in endothelial cells in lesions [30]. However, binding to VCAM-1 was equal in both cell types upon oxLDL treatment, suggesting that in the setting of atherosclerosis (i.e., in conditions where oxLDL is present), the presence of hAIM may not greatly contribute to an increase in macrophage binding to VCAM-1. Overall, these data suggest that hAIM may contribute to macrophage-endothelial cell adhesion. To our knowledge, modulation of macrophage-endothelial interactions by hAIM is an unprecedented function of this protein, and we are studying this phenomenon further.

Foam cells are the hallmark of atherosclerosis development. Assessment of oxLDL foam cell formation evidenced an additional, new role for hAIM by enhancing macrophage lipid storage. Increased cell cholesterol accumulation could be a result of a decreased efflux, increased uptake, or both. Therefore, the efflux of cholesterol was the next factor evaluated as a potential mechanism involved in the macrophage accumulation of lipids induced by hAIM. Real-time PCR experiments showed that the mRNA levels of the transporter ABCG1, but not those of ABCA1, were increased significantly in hAIM-expressing cells. Consistently, our data show that cholesterol efflux to apoA-I (the ABCA1 acceptor) in THP1 cells and HMDMs was not modified in the presence of hAIM. In addition, we found that hAIM-mediated overexpression of the ABCG1 transporter was associated with an increase in cholesterol efflux from macrophages to its acceptor (mature HDL) in THP1 cells. However, we did not detect a similar effect on HMDMs in parallel, independent experiments. Thus, overall, hAIM does not seem to play a major role in cholesterol efflux to HDL. To confirm this notion, we also tested that cholesterol efflux was not changed when plasma was used as a cholesterol acceptor. Considering that plasma is the most complex and yet most physiological cholesterol acceptor for the wide spectrum of lipoproteins and apolipoproteins present in this milieu, these results further confirm a minimal contribution, if any, of this pathway in cholesterol accumulation in macrophages.

In fact, our findings suggest that increased foam cell formation by hAIM is mainly a result of increased lipid uptake. It has been reported recently that mAIM binds to cell-surface CD36 and uses it as an endocytic receptor to enter adipocytes and macrophages [21]. With these data in mind and as CD36 is one of the major scavenger receptors for oxLDL, we hypothesized that hAIM may be increasing oxLDL uptake by modulating CD36 expression and/or activity. Indeed, hAIM expression induced the up-regulation of CD36 mRNA levels in THP1-hAIM-expressing versus THP1-vector cells, which increased further upon oxLDL treatment. Also, addition of rhAIM to HMDMs increased CD36 cell-surface expression in these cells by twofold compared with control Alb protein.

We then tested whether hAIM could serve as a soluble protein that binds to oxLDL. rhAIM showed dose-dependent and saturable binding to oxLDL in direct ELISA as-

says. The binding of hAIM to oxLDL is of relevance, as this protein is composed of SRCR domains exclusively. This domain consists of ~100 aa containing six to eight cysteine residues with a well-conserved disulfide bond pattern [15, 48]. The SRCR domain is present in proteins that play relevant roles in lipid binding and homeostasis, such as macrophage SR-AI [49] and macrophage receptor with collagenous structure [50, 51]. However, to our knowledge, the SRCR domain has never been proven to interact with oxLDL. The high degree of structural and phylogenetic conservation of the SRCR domains has helped elucidate several common functions among the SRCR proteins, such as binding to bacteria [15, 52–54]. The finding that hAIM binds to oxLDL opens the possibility that other SRCR proteins may as well bind to this mLDL.

Binding of rhAIM to oxLDL suggested that it may serve as a soluble protein that transfers oxLDL to CD36. This was tested in a widely used in vitro system in HEK-293 cells [2, 4]. When CD36-expressing HEK-293 cells were treated with rhAIM, an increase in oxLDL uptake compared with Alb-treated cells was appreciated. Therefore, our results suggest that hAIM serves to facilitate CD36-mediated uptake of oxLDL in HEK-293 cells. Furthermore, silencing of cell-surface expression of CD36 by specific siRNA transfection inhibited THP1 cell uptake of oxLDL, reinforcing the notion that uptake is mediated, at least in part, through this receptor. Our data are in agreement with previous reports that have shown that lack of CD36 expression or blocking of CD36 binding sites with a specific antibody (OKM5) reduced 40–50% macrophage binding and uptake of oxLDL [3, 55]. All in all, these results, together with induced CD36 expression, could explain enhanced oxLDL uptake by macrophages in the presence of hAIM. However, they do not discard a possible contribution of other oxLDL scavenger receptors, such as SR-BI.

Several functions of hAIM in macrophage biology that are described in this study, such as LFA-1, Mac-1, and CD36 overexpression, occur independently of oxLDL lipid uptake. Given that Iwamura et al. [22] showed that mAIM decreased FASN activity in adipocytes, we tested whether this effect could be associated with hAIM-induced up-regulation of these receptors. Our data indicated that treatment of THP1 cells with C75, a synthetic FASN inhibitor, diminished cell-surface expression of CD18, CD11a, and CD11b, whereas not significantly affecting that of CD36. Therefore, inhibition of FASN activity does not modulate cell-surface expression of these receptors in a similar way as hAIM does, and it cannot account for the effects of hAIM. Further studies are underway to analyze the mechanisms by which hAIM enhances LFA-1, Mac-1, and CD36 expression in macrophages.

In summary, our results support the notion that hAIM is an atherogenic protein that participates in multiple events of macrophage homeostasis, including macrophage survival, adhesion to endothelial ICAM-1 and VCAM-1, as well as oxLDL uptake and subsequent foam cell formation. Our findings are of relevance for the understanding of key cellular events that contribute to atherosclerosis.

AUTHORSHIP

N.A. and M-R.S. initiated the study, analyzed the data, and wrote the manuscript. J.J., J.C.E-G., and F.B-V. contributed to the lipid homeostasis assays. N.A., L.S., and G.A. contributed to most of the experimental part. B.P-C., P.B-A., and F.E.B. contributed to HMDM isolation and characterization. R.V. provided mAb and together with J.J., J.C.E-G., C.A., F.E.B., and A.F.V., helped in the analysis, interpretation, and writing of the manuscript.

ACKNOWLEDGMENTS

This work was supported by grants from Fundació Marató de TV3, MTV308932, and Ministerio de Sanidad y Consumo, Instituto de Salud Carlos III, FIS PI10/1565 (to M-R.S.), FIS 100277 (to J.J.), 110176 (to F.B-V.), and 090178 (to J.C.E-G.). M-R.S. is supported by the Miguel Servet Research Program (CP08/124) and C.A., by a Ramon y Cajal fellowship (RYC-2010–07249). We thank Marco Fernandez, Pilar Armengol, Gerard Requena, and Eugeni Aragall (Flow Cytometry, Genetics and Microscopy Units, IGTP) for their technical support and Tanya Yates for English corrections.

DISCLOSURES

The authors declare no conflict of interest.

REFERENCES

1. Silverstein, R. L. (2009) Inflammation, atherosclerosis, and arterial thrombosis: role of the scavenger receptor CD36. *Cleve. Clin. J. Med.* **76**, S27–S30.
2. Kunjathoor, V. V., Febbraio, M., Podrez, E. A., Moore, K. J., Andersson, L., Koehn, S., Rhee, J. S., Silverstein, R., Hoff, H. F., Freeman, M. W. (2002) Scavenger receptors class A-I/II and CD36 are the principal receptors responsible for the uptake of modified low density lipoprotein leading to lipid loading in macrophages. *J. Biol. Chem.* **277**, 49982–49988.
3. Febbraio, M., Podrez, E. A., Smith, J. D., Hajjar, D. P., Hazen, S. L., Hoff, H. F., Sharma, K., Silverstein, R. L. (2000) Targeted disruption of the class B scavenger receptor CD36 protects against atherosclerotic lesion development in mice. *J. Clin. Invest.* **105**, 1049–1056.
4. Endemann, G., Stanton, L. W., Madden, K. S., Bryant, C. M., White, R. T., Protter, A. A. (1993) CD36 is a receptor for oxidized low density lipoprotein. *J. Biol. Chem.* **268**, 11811–11816.
5. Hoebe, K., Georgel, P., Rutschmann, S., Du, X., Mudd, S., Crozat, K., Sovath, S., Shamel, L., Hartung, T., Zahring, U., Beutler, B. (2005) CD36 is a sensor of diacylglycerides. *Nature* **433**, 523–527.
6. Mikołajczyk, T. P., Skrzeczynska-Moncznik, J. E., Zarębski, M. A., Marewicz, E. A., Wiśniewska, A. M., Dzięba, M., Dobrucki, J. W., Pryjma, J. R. (2009) Interaction of human peripheral blood monocytes with apoptotic polymorphonuclear cells. *Immunology* **128**, 103–113.
7. Savill, J., Hogg, N., Ren, Y., Haslett, C. (1992) Thrombospondin cooperates with CD36 and the vitronectin receptor in macrophage recognition of neutrophils undergoing apoptosis. *J. Clin. Invest.* **90**, 1513–1522.
8. Schmitz, G., Langmann, T., Heimerl, S. (2001) Role of ABCG1 and other ABCG family members in lipid metabolism. *J. Lipid Res.* **42**, 1513–1520.
9. Jessup, W., Gelissen, I. C., Gaus, K., Kritharides, L. (2006) Roles of ATP binding cassette transporters A1 and G1, scavenger receptor BI and membrane lipid domains in cholesterol export from macrophages. *Curr. Opin. Lipidol.* **17**, 247–257.
10. Asztalos, B. F., Roheim, P. S. (1995) Presence and formation of 'free apolipoprotein A-I-like' particles in human plasma. *Arterioscler. Thromb. Vasc. Biol.* **15**, 1419–1423.
11. Rothblat, G. H., de la Llera-Moya, M., Atger, V., Kellner-Weibel, G., Williams, D. L., Phillips, M. C. (1999) Cell cholesterol efflux: integration of old and new observations provides new insights. *J. Lipid Res.* **40**, 781–796.
12. Fielding, C. J., Fielding, P. E. (1995) Molecular physiology of reverse cholesterol transport. *J. Lipid Res.* **36**, 211–228.
13. Lusis, A. J. (2000) Atherosclerosis. *Nature* **407**, 233–241.

14. Lusis, A. J., Mar, R., Pajukanta, P. (2004) Genetics of atherosclerosis. *Annu. Rev. Genomics Hum. Genet.* **5**, 189–218.
15. Sarrias, M. R., Gronlund, J., Padilla, O., Madsen, J., Holmskov, U., Lozano, F. (2004) The scavenger receptor cysteine-rich (SRCR) domain: an ancient and highly conserved protein module of the innate immune system. *Crit. Rev. Immunol.* **24**, 1–37.
16. Joseph, S. B., Bradley, M. N., Castrillo, A., Bruhn, K. W., Mak, P. A., Pei, L., Hogenesch, J., O'Connell, R. M., Cheng, G., Saez, E., Miller, J. F., Tontonoz, P. (2004) LXR-dependent gene expression is important for macrophage survival and the innate immune response. *Cell* **119**, 299–309.
17. Valledor, A. F., Hsu, L. C., Ogawa, S., Sawka-Verhelle, D., Karin, M., Glass, C. K. (2004) Activation of liver X receptors and retinoid X receptors prevents bacterial-induced macrophage apoptosis. *Proc. Natl. Acad. Sci. USA* **101**, 17813–17818.
18. Arai, S., Shelton, J. M., Chen, M., Bradley, M. N., Castrillo, A., Bookout, A. L., Mak, P. A., Edwards, P. A., Mangelsdorf, D. J., Tontonoz, P., Miyazaki, T. (2005) A role for the apoptosis inhibitory factor AIM/Spα/Api6 in atherosclerosis development. *Cell Metab.* **1**, 201–213.
19. Haruta, I., Kato, Y., Hashimoto, E., Minjares, C., Kennedy, S., Uto, H., Yamauchi, K., Kobayashi, M., Yusa, S., Muller, U., Hayashi, N., Miyazaki, T. (2001) Association of AIM, a novel apoptosis inhibitory factor, with hepatitis via supporting macrophage survival and enhancing phagocytotic function of macrophages. *J. Biol. Chem.* **276**, 22910–22914.
20. Kuwata, K., Watanabe, H., Jiang, S. Y., Yamamoto, T., Tomiyama-Miyaji, C., Abo, T., Miyazaki, T., Naito, M. (2003) AIM inhibits apoptosis of T cells and NKT cells in Corynebacterium-induced granuloma formation in mice. *Am. J. Pathol.* **162**, 837–847.
21. Kurokawa, J., Arai, S., Nakashima, K., Nagano, H., Nishijima, A., Miyata, K., Ose, R., Mori, M., Kubota, N., Kadowaki, T., Oike, Y., Koga, H., Febbraio, M., Iwanaga, T., Miyazaki, T. (2010) Macrophage-derived AIM is endocytosed into adipocytes and decreases lipid droplets via inhibition of fatty acid synthase activity. *Cell Metab.* **11**, 479–492.
22. Iwamura, Y., Mori, M., Nakashima, K., Mikami, T., Murayama, K., Arai, S., Miyazaki, T. (2012) Apoptosis inhibitor of macrophage (AIM) diminishes lipid droplet-coating proteins leading to lipolysis in adipocytes. *Biochem. Biophys. Res. Commun.* **422**, 476–481.
23. Naranjo-Gómez, M., Fernández, M. A., Bofill, M., Singh, R., Navarrete, C. V., Pujol-Borrell, R., Borrás, F. E. (2005) Primary alloproliferative TH1 response induced by immature plasmacytoid dendritic cells in collaboration with myeloid DCs. *Am. J. Transplant.* **5**, 2838–2848.
24. Julve, J., Escola-Gil, J. C., Rotllan, N., Firvet, C., Vallez, E., de la Torre, C., Ribas, V., Sloan, J. H., Blanco-Vaca, F. (2011) Human apolipoprotein A-II determines plasma triglycerides by regulating lipoprotein lipase activity and high-density lipoprotein proteome. *Arterioscler. Thromb. Vasc. Biol.* **30**, 232–238.
25. Ziouzenkova, O., Sevanian, A., Abuja, P. M., Ramos, P., Esterbauer, H. (1998) Copper can promote oxidation of LDL by markedly different mechanisms. *Free Radic. Biol. Med.* **24**, 607–623.
26. Kritharides, L., Christian, A., Stoudt, G., Morel, D., Rothblat, G. H. (1998) Cholesterol metabolism and efflux in human THP-1 macrophages. *Arterioscler. Thromb. Vasc. Biol.* **18**, 1589–1599.
27. Fraser, D. A., Tenner, A. J. (2010) Innate immune proteins C1q and mannans-binding lectin enhance clearance of atherogenic lipoproteins by human monocytes and macrophages. *J. Immunol.* **185**, 3932–3939.
28. Galkina, E., Ley, K. (2007) Vascular adhesion molecules in atherosclerosis. *Arterioscler. Thromb. Vasc. Biol.* **27**, 2292–2301.
29. Roebuck, K. A., Finnegan, A. (1999) Regulation of intercellular adhesion molecule-1 (CD54) gene expression. *J. Leukoc. Biol.* **66**, 876–888.
30. Galkina, E., Ley, K. (2007) Vascular adhesion molecules in atherosclerosis. *Arterioscler. Thromb. Vasc. Biol.* **27**, 2292–2301.
31. Tabas, I. (2000) Cholesterol and phospholipid metabolism in macrophages. *Biochim. Biophys. Acta* **1529**, 164–174.
32. Xu, M., Zhou, H., Tan, K. C., Guo, R., Shiu, S. W., Wong, Y. (2009) ABCG1 mediated oxidized LDL-derived oxysterol efflux from macrophages. *Biochem. Biophys. Res. Commun.* **390**, 1349–1354.
33. De la Llera-Moya, M., Rothblat, G. H., Connelly, M. A., Kellner-Weibel, G., Sakr, S. W., Phillips, M. C., Williams, D. L. (1999) Scavenger receptor BI (SR-BI) mediates free cholesterol flux independently of HDL tethering to the cell surface. *J. Lipid Res.* **40**, 575–580.
34. Han, J., Hajjar, D. P., Febbraio, M., Nicholson, A. C. (1997) Native and modified low density lipoproteins increase the functional expression of the macrophage class B scavenger receptor, CD36. *J. Biol. Chem.* **272**, 21654–21659.
35. Hayden, J. M., Brachova, L., Higgins, K., Obermiller, L., Sevanian, A., Khandrika, S., Reaven, P. D. (2002) Induction of monocyte differentiation and foam cell formation in vitro by 7-ketocholesterol. *J. Lipid Res.* **43**, 26–35.
36. Gebe, J. A., Kiener, P. A., Ring, H. Z., Li, X., Francke, U., Aruffo, A. (1997) Molecular cloning, mapping to human chromosome 1 q21-q23, and cell binding characteristics of Spα, a new member of the scavenger receptor cysteine-rich (SRCR) family of proteins. *J. Biol. Chem.* **272**, 6151–6158.
37. Gebe, J. A., Llewellyn, M., Hoggatt, H., Aruffo, A. (2000) Molecular cloning, genomic organization and cell-binding characteristics of mouse Spα. *Immunology* **99**, 78–86.
38. Sarrias, M. R., Padilla, O., Monreal, Y., Carrascal, M., Abian, J., Vives, J., Yelamos, J., Lozano, F. (2004) Biochemical characterization of recombinant and circulating human Spα. *Tissue Antigens* **63**, 335–344.
39. Mori, M., Kimura, H., Iwamura, Y., Arai, S., Miyazaki, T. (2012) Modification of N-glycosylation modulates the secretion and lipolytic function of apoptosis inhibitor of macrophage (AIM). *FEBS Lett.* **586**, 3569–3574.
40. McLaren, J. E., Michael, D. R., Ashlin, T. G., Ramji, D. P. (2011) Cytokines, macrophage lipid metabolism and foam cells: implications for cardiovascular disease therapy. *Prog. Lipid Res.* **50**, 331–347.
41. Miyazaki, T., Hirokami, Y., Matsuhashi, N., Takatsuka, H., Naito, M. (1999) Increased susceptibility of thymocytes to apoptosis in mice lacking AIM, a novel murine macrophage-derived soluble factor belonging to the scavenger receptor cysteine-rich domain superfamily. *J. Exp. Med.* **189**, 413–422.
42. Hegyi, L., Hardwick, S. J., Siow, R. C., Skepper, J. N. (2001) Macrophage death and the role of apoptosis in human atherosclerosis. *J. Hematother. Stem Cell Res.* **10**, 27–42.
43. Hamilton, J. A., Myers, D., Jessup, W., Cochrane, F., Byrne, R., Whitty, G., Moss, S. (1999) Oxidized LDL can induce macrophage survival, DNA synthesis, and enhanced proliferative response to CSF-1 and GM-CSF. *Arterioscler. Thromb. Vasc. Biol.* **19**, 98–105.
44. Hundal, R. S., Gomez-Munoz, A., Kong, J. Y., Salh, B. S., Marotta, A., Duronio, V., Steinbrecher, U. P. (2003) Oxidized low density lipoprotein inhibits macrophage apoptosis by blocking ceramide generation, thereby maintaining protein kinase B activation and Bcl-XL levels. *J. Biol. Chem.* **278**, 24399–24408.
45. Biwa, T., Hakamata, H., Sakai, M., Miyazaki, A., Suzuki, H., Kodama, T., Shichiri, M., Horiuchi, S. (1998) Induction of murine macrophage growth by oxidized low density lipoprotein is mediated by granulocyte macrophage colony-stimulating factor. *J. Biol. Chem.* **273**, 28305–28313.
46. Nakashima, Y., Raines, E. W., Plump, A. S., Breslow, J. L., Ross, R. (1998) Upregulation of VCAM-1 and ICAM-1 at atherosclerosis-prone sites on the endothelium in the ApoE-deficient mouse. *Arterioscler. Thromb. Vasc. Biol.* **18**, 842–851.
47. Jeng, J. R., Chang, C. H., Shieh, S. M., Chiu, H. C. (1993) Oxidized low-density lipoprotein enhances monocyte-endothelial cell binding against shear-stress-induced detachment. *Biochim. Biophys. Acta* **1178**, 221–227.
48. Freeman, M., Ashkenas, J., Rees, D. J., Kingsley, D. M., Copeland, N. G., Jenkins, N. A., Krieger, M. (1990) An ancient, highly conserved family of cysteine-rich protein domains revealed by cloning type I and type II murine macrophage scavenger receptors. *Proc. Natl. Acad. Sci. USA* **87**, 8810–8814.
49. Bowdish, D. M., Gordon, S. (2009) Conserved domains of the class A scavenger receptors: evolution and function. *Immunol. Rev.* **227**, 19–31.
50. Doi, T., Higashino, K., Kurihara, Y., Wada, Y., Miyazaki, T., Nakamura, H., Uesugi, S., Imanishi, T., Kawabe, Y., Itakura, H. (1993) Charged collagen structure mediates the recognition of negatively charged macromolecules by macrophage scavenger receptors. *J. Biol. Chem.* **268**, 2126–2133.
51. Tanaka, T., Nishikawa, A., Tanaka, Y., Nakamura, H., Kodama, T., Imanishi, T., Doi, T. (1996) Synthetic collagen-like domain derived from the macrophage scavenger receptor binds acetylated low-density lipoprotein in vitro. *Protein Eng.* **9**, 307–313.
52. Elomaa, O., Kangas, M., Sahlberg, C., Tuukkanen, J., Sormunen, R., Liakka, A., Thesleff, I., Kraal, G., Tryggvason, K. (1995) Cloning of a novel bacteria-binding receptor structurally related to scavenger receptors and expressed in a subset of macrophages. *Cell* **80**, 603–609.
53. Fabrick, B. O., van Bruggen, R., Deng, D. M., Ligtenberg, A. J., Nazmi, K., Schornagel, K., Vloet, R. P., Dijkstra, C. D., van den Berg, T. K. (2009) The macrophage scavenger receptor CD163 functions as an innate immune sensor for bacteria. *Blood* **113**, 887–892.
54. Sarrias, M. R., Farnos, M., Mota, R., Sanchez-Barbero, F., Ibanez, A., Gimferrer, I., Vera, J., Fenutria, R., Casals, C., Yelamos, J., Lozano, F. (2007) CD6 binds to pathogen-associated molecular patterns and protects from LPS-induced septic shock. *Proc. Natl. Acad. Sci. USA* **104**, 11724–11729.
55. Nozaki, S., Kashiwagi, H., Yamashita, S., Nakagawa, T., Kostner, B., Tomiyama, Y., Nakata, A., Ishigami, M., Miyagawa, J., Kameda-Takemura, K., et al. (1995) Reduced uptake of oxidized low density lipoproteins in monocyte-derived macrophages from CD36-deficient subjects. *J. Clin. Invest.* **96**, 1859–1865.

KEY WORDS:

CD5L · Spα · macrophage · atherosclerosis · apoptosis